Observations of a Geosynchronous Satellite with Optical Interferometry

J. T. Armstrong, R. B. Hindsley, S. R. Restaino
Naval Research Laboratory
J. A. Benson, D. J. Hutter, F. J. Vrba, R. T. Zavala
U. S. Naval Observatory
S. A. Gregory
Boeing LTS, Inc.
H. R. Schmitt
Interferometrics, Inc.

ABSTRACT

We report an interferometric detection of an earth-orbiting artificial satellite using optical interferometry. We targeted four geosynchronous communications satellites with the Navy Prototype Optical Interferometer (NPOI) near Flagstaff, AZ, and obtained interferometric fringes on one of them, DIRECTV-9S. We used an east-west 15.9-meter baseline of the NPOI and took data in 16 spectral channels covering the 500-850 nm wavelength range. Observations took place during the "glint season" of 28 February to 3 March 2008, and then again in February-March 2009, when the geometry of the solar panel arrays and the Sun's position creates glints as bright as 2nd magnitude of a few minutes' duration each night. We detected fringes on the satellite at approximately the 2 sigma level on 1 March at magnitude 4.5. Subsequent analysis shows that the fringe amplitudes are consistent with a size scale of 2 meters (50 nanoradians at GEO) in an east-west direction. This detection shows that interferometric detection of satellites at visual wavelengths is possible, and suggests that a multi-baseline interferometer array tailored to the angular size and brightness of geosynchronous satellites could lead to images of these satellites.

1. INTRODUCTION

Geosynchronous satellites are a critical component of modern communications, surveillance, and environmental and weather observation. However, monitoring the orientations and configurations of these satellites is difficult because of their faintness and small angular size: at most times, the brightness of typical communications satellites is about 12^m to 14^m, while a 2 m $\times$ 40 m solar panel array subtends 0.01×0.2 arc sec (= 10×200 milliarcsec [mas] = 0.05×1 μrad), a resolution that is at the limits of most adaptive optics (AO) systems.

Optical/infrared interferometry (OI) offers the possibility of overcoming the resolution limits of single telescopes. This technology, which combines light beams from individual telescopes separated by distances from tens to hundreds of meters, has been under development for astronomical observations since the pioneering work of Michelson in the early 20th century. This development has accelerated in the past 10–15 years with the advent of multi-telescope arrays with complex beam-combining systems. The most recent developments can be found in [1]. The Navy Prototype Optical Interferometer (NPOI), located at the Lowell Observatory site near Flagstaff, AZ, is one of the leading optical interferometers currently in operation, observing at visual wavelengths (450—800 nm) with up to six telescopes on baselines (i.e., telescope separations) up to 79 m [2, 3].

The primary limitation of current OI instruments is sensitivity: most interferometers operating in the visual and near-infrared bands can reach 5^m to 7^m, considerably short of the sensitivity needed to observe GEO satellites during most of the year. A secondary difficulty is, oddly, too much resolution: most current instruments have minimum baselines of 15 m or more. For observations at visual wavelengths, this length is enough to "resolve out" any structure in geosynchronous orbit larger than ~2 m. Image structure larger than that produces interference fringes that are too weak to detect within the atmospheric coherence time of ~10 ms.

In this paper, we present a tentative interferometric detection of a satellite with optical interferometry during "glint" season—when some geosynchronous satellites briefly reach magnitudes as bright as 2 or 3—using a baseline of just over 15 m. The technique of optical interferometry is described in Section 2, the NPOI in particular in Section 3,

our observations in Section 4, the size of the glinting area and the satellite spectrum in Section 5, high-precision position measurements in Section 6, and planned follow-up work in Section 7.

2. OPTICAL INTERFEROMETRY

Michelson's implementation of optical interferometry involved placing a mask with two holes over the aperture of a conventional telescope, as shown in Fig. 1. Each of the two subapertures separated by a distance B admits a portion of the light wave from the target. A single subaperture produces an image with a diffraction width of $\Delta\theta \sim \lambda/D$, while the two beams interfering in the focal plane of the telescope produce interference fringes whose width is $\delta\theta \sim \lambda/B$. The interferometric combination thus increases the angular resolution by a factor B/D.
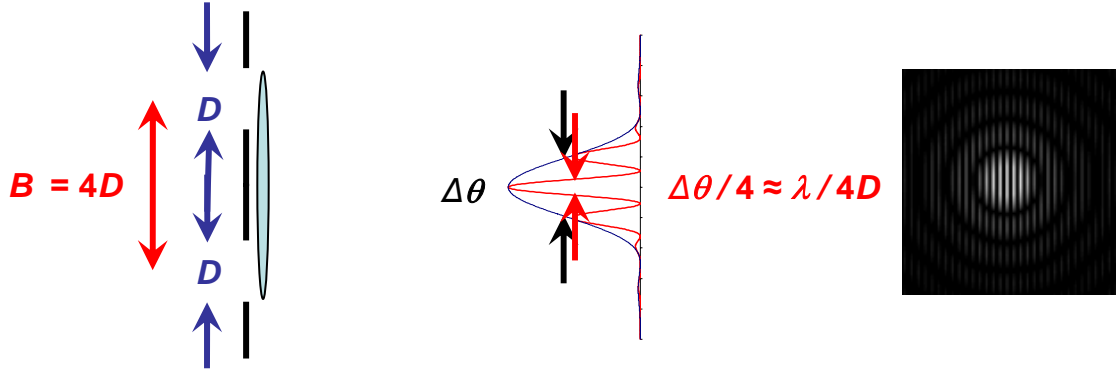

Fig. 1. A schematic diagram of the principle of interferometric imaging. In this example, a mask with two holes of diameter D are placed in front of a telescope with a separation of $B = 4D$. If the target is a point source, each of the holes produces an image of angular size $\Delta\theta = \lambda/D$ in the focal plane. Interference between the two beams entering via the subapertures produces bright and dark interference fringes across this image, as shown on the right. The width of a fringe is $\Delta\theta/4$, so the imaging resolution of the pair of subapertures is four times the resolution of each subaperture by itself.

The largest telescope apertures are currently 10 m across, but resolving images of stars, typically a few milliseconds of arc (1 mas, which is approximately 5 nanoradians) in size, requires aperture separations of tens to hundreds of meters at visual wavelengths. As a result, modern interferometers dispense with masked apertures, substituting individual telescopes that send light to a central optics laboratory. These telescopes can then be separated by much larger distances than would be possible in a single masked aperture. The transfer and beam combining optics of the interferometer are configured to treat the light as if it were received and focused by a single masked telescope. A schematic diagram of a simple two-element interferometer is shown in Fig. 2.

In practice, as many as six telescopes have been used simultaneously to produce multiple sets of interference fringes. Fringe strength on different baselines varies, depending on the size and structure of the target. The strengths of these fringe systems, along with instrument configuration information such as telescope positions and the observing wavelength(s), are used to compute the characteristics of the target. In particular, the square of the fringe visibility, a measure of the contrast between the bright and dark areas of a fringe pattern, for a uniformly-bright disk is given by

$$V^2 = \frac{2J_1(\pi\theta \cdot B/\lambda)}{\pi\theta \cdot B/\lambda},$$

where $J_1(x)$ is a Bessel function of the first kind, θ is the angular diameter of the disk, B is the telescope separation, and λ is the observing wavelength. The combination B/λ, known as the spatial frequency, is the inverse of the resolution of the interferometer. In observations with a given baseline B over a range of wavelengths, the interferometer samples a range of spatial frequencies. For partially-resolved targets like the geosynchronous satellites in our program, V^2 decreases as the wavelength becomes shorter.
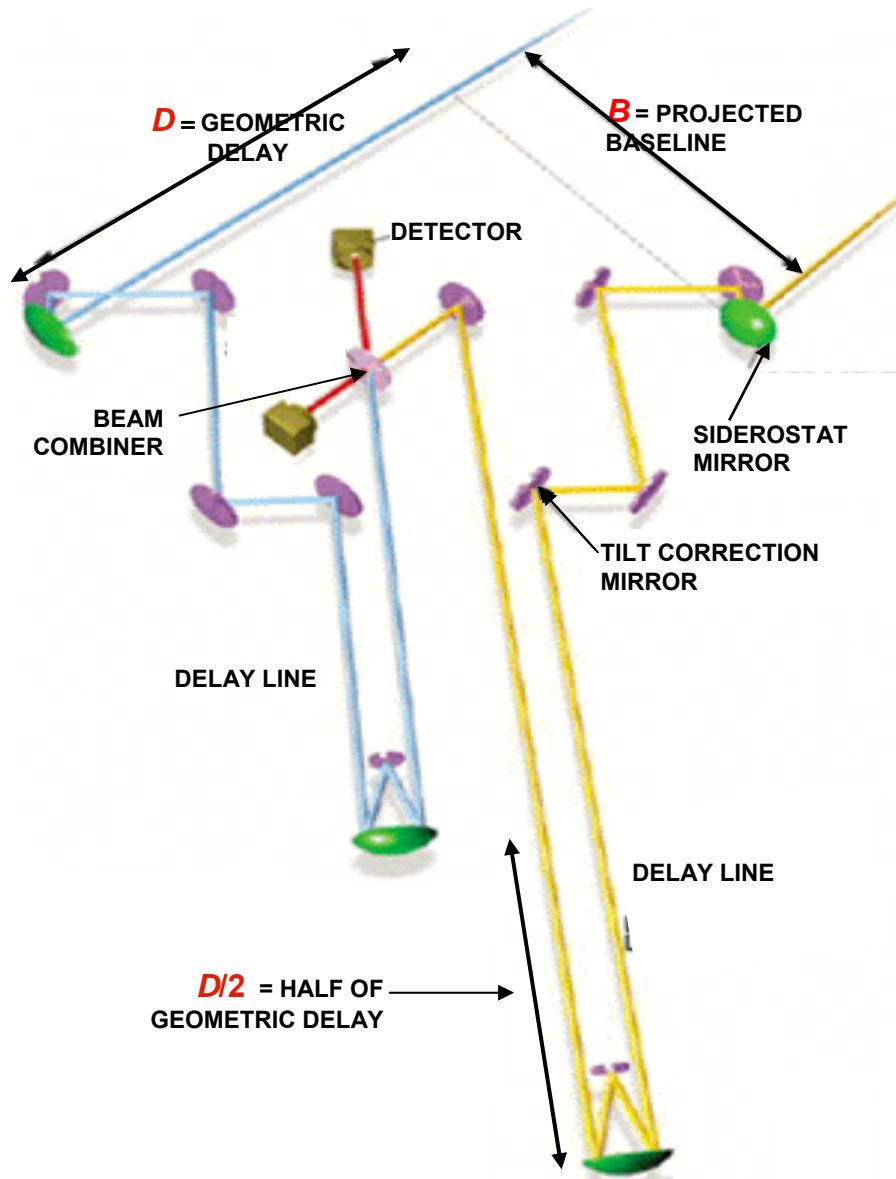
Fig. 2. Schematic diagram of a simple two-element interferometer. The imaging target is out of the diagram, above and to the right, and is closer to the right-hand aperture than to the left by the geometric delay, D. In this example, siderostats (flat mirrors that direct light into the optical train of the interferometer) are used rather than telescopes. The delay lines compensate for the geometric delay, ensuring that the portions of the incoming wavefront received by the two siderostats arrive simultaneously at the beam combiner so interference can take place.

3. THE NAVY PROTOTYPE OPTICAL INTERFEROMETER

The Navy Prototype Optical Interferometer (NPOI) [2], a joint project of the Naval Research Laboratory and the US Naval Observatory in partnership with the Lowell Observatory, is located at the Lowell Observatory site on Anderson Mesa, near Flagstaff, Arizona. Its design comprises two arrays: one array of four siderostats at fixed locations for astrometry, i.e., precise measurements of stellar positions, and a second array of moveable siderostats for stellar imaging. The astrometric-array siderostats are equipped with laser metrology for precise monitoring of the array geometry, which is required for astrometry at the 1 to 10 mas level. The imaging siderostats can be moved among 30 stations on the array, with station separations ranging from 2.5 m to 437 m. Two imaging siderostats are now in operation; they can be used with the four astrometric siderostats to make a six-element imaging array. The

arrays share an optics laboratory that contains the delay lines and the beam combiner, and a vacuum feed pipe system to convey light from the siderostats to the optics lab.

The current configuration of the NPOI consists of the four astrometric siderostats, plus two of the imaging siderostats. Baseline lengths in the current layout range from 18.9 m to 38.2 m for the astrometric array, and 15.9 m to 79 m for the imaging array, with a 98 m baseline expected to become available in early 2009. The detectors cover a wavelength range of 550 to 850 nm in 16 spectral channels. With these wavelengths, the NPOI's baselines can resolve targets from 1.3 mas to 30 mas (7 nrad to 150 nrad) in size, over a field of view of 0.2". Targets larger than 30 mas are "resolved out"; the fringe visibility becomes too low for detection. Targets smaller than ~1.3 mas are unresolved and thus appear as point sources.

The NPOI siderostats are 40 cm in diameter, but only 12 cm of these apertures are used, due to the mirror diameters in the vacuum feed pipe system. As a result of the aperture size, the NPOI's maximum sensitivity is about magnitude 5.5 in the R wavelength band (centered near 700 nm). Beam-compressing telescopes (35 cm apertures) have been obtained for the astrometric siderostats and should increase the sensitivity by 1 to 2 magnitudes when they are installed. USNO has also obtained four 1.8 m telescopes formerly designated for the Keck Observatory interferometer on Mauna Kea, Hawaii. They would be installed at the NPOI at fixed locations, with baseline lengths ranging from ~50 m to ~150 m. An NRL 6.2 program has developed a lightweight 1.4 m telescope based on carbon fiber reinforced polymer (CFRP) that demonstrates the feasibility of using such telescopes as moveable imaging-array elements. Both types of larger aperture would improve sensitivity by 3 to 4 magnitudes.

The NPOI has been used for a variety of astrophysical imaging projects since it saw first fringes in 1994, such as measuring double-star and triple-star orbits [4]; measuring diameters of stars, including the pulsating Cepheid variables used as standard candles in the nearby parts of extragalactic space [5], and observing the oblate shapes of such rapidly rotating stars as Vega [6] and Altair. The astrometric array is currently embarked on producing a catalog of stellar positions with 10 mas accuracy or better.

4. NPOI OBSERVATIONS OF GEOSTATIONARY SATELLITES

Observations of geostationary satellites with the NPOI are constrained by three important considerations. The first is sensitivity. The typical brightness of these satellites during most of the year is ~12 to 14 mag [7], or very roughly a factor of 1000 too faint for the NPOI (five magnitudes is a factor of 100 in flux). However, satellites with large solar-panel arrays (many of them are ~2 m wide by up to 40 m long) can glint brightly at certain times of the year, a few of them as bright as 4 mag or brighter. The timing of the glints depends on the relative positions of the Sun and the satellite, on the satellite orientation, and on the departure of the solar arrays from perfect flatness. Because the panels are usually oriented north-south, the glints take place just before the spring equinox and just after the fall equinox, when the topocentric declination of the satellite and the declination of the Sun are approximately equal, creating an opportunity for an observer to see the Sun reflected in the solar panels. Within its glint season, which lasts about a week, a satellite glints each night for a period of ~5 to 20 min.

Our second constraint is baseline length. Our shortest current baseline is 15.9 m, corresponding to a resolution of ~10 mas (50 nrad, or 1.8 m at geosynchronous distance) at 800 nm wavelength. The long dimension of the panels, 20 to 40 m, is too large for that baseline: a target that size is resolved out, as mentioned above. Fortunately, our 15.9 m baseline is oriented east-west, so it is sensitive to the width of the panels. The typical width of ~2 m is just small enough for us to detect, although the fringe visibility would be low. The fringe visibility will be higher if only smaller parts of the panels glint at a given time, as seems likely.

The third constraint is the need to know the satellite position. In order to set the NPOI's delay lines close to the positions needed to produce fringes at the beam combiner, we need to know the satellite position to within 1" or better; otherwise, the range of delay-line positions over which the NPOI would have to search would be too large to cover in the 5 to 20 min. duration of the glint. We can calculate positions from the orbital elements ("three-line elements," or TLEs), which are available on line [8] and are updated every few days, but those positions are precise only at the level of a few arcsec, and the satellite operators can move their satellites at any time.

With these constraints in mind, we have attempted interferometric detection of geostationary satellites with the NPOI on two occasions. On both occasions, we used the Naval Observatory Flagstaff Station (NOFS) 40-inch

telescope to measure the satellite positions. The NOFS observations are challenging partly because stars appear as streaks in the astrometric frames, and partly because a glinting satellite is much brighter than the reference stars.

Our first attempt with the NPOI took place in October 2007. We observed five satellites, but we did not detect fringes for any of them. We concluded that the likely cause for our nondetections was that the satellite positions from our NOFS observations were not accurate enough.

With the experience we gained in October 2007 and with improvements in our astrometry techniques, we tried again from 27 February to 4 March 2008. We monitored the brightnesses of eight satellites and searched for fringes on four of them: DIRECTV-9S, ANIK-F1R, GALAXY 10R, and DIRECTV-4S. We lost one night to clouds and one to wind. Two nights, however, had good "seeing" (i.e., steady images).

At 0537 UT on 1 March 2008, we detected interference fringes on the 15.9 m baseline between the Astrometric East (AE) and East-6 (E6) siderostats while observing DIRECTV-9S. We did not detect fringes on the second baseline in use that night, the 18.9 m AE to Astrometric Center (AC) baseline. The effective lengths of the baselines, correcting for projection effects toward the satellite, were 15.0 m for AE-E6 and 18.9 m for AE-AC. Fig. 3 shows the real-time fringe signal-to-noise ratio and photon rate monitors at the time of detection. The fringes were ~3 times the noise floor over a period of about 5 s. We have only a rough measure of the brightness, magnitude ~4 to 5, of the satellite at the time the fringes were detected.
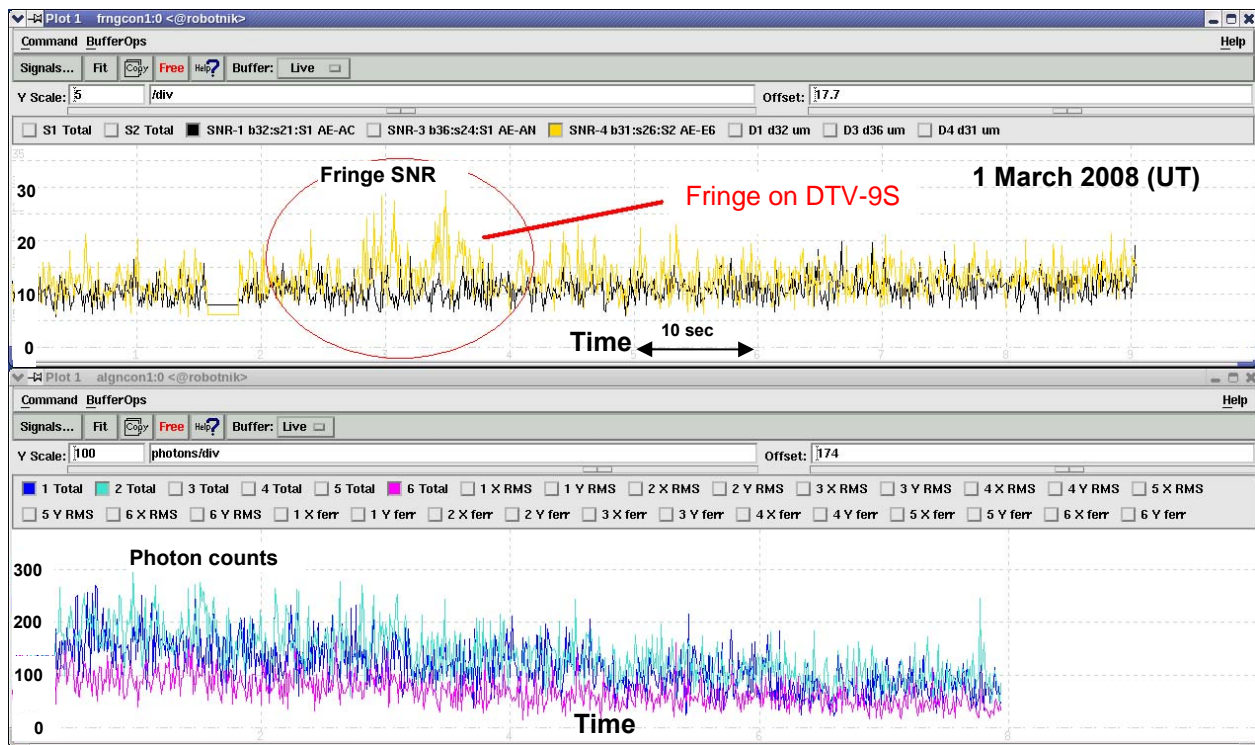

Fig. 3. Tentative first detection of fringes in an observation of a satellite. The upper panel shows the fringe visibility signal-to-noise ratio for the two baselines used in these observations. (The SNR here is un-normalized, so a value of 10 is the noise level.) The yellow trace corresponds to the 15.9 m baseline between the Astrometric East (AE) and East-6 (E6) siderostats. The lower panel shows the photon counts per second on the star-tracking detectors for each of the three siderostats in use. Below a rate of ~200 s^{-1}, fringe detection becomes difficult.

5. SIZE SCALE OF GLINTING AREA, AND SPECTRUM VARIATIONS

Because of the low fringe SNR, we characterize this detection as tentative. With that caveat in mind, in this section we treat it as a real detection and discuss the conclusions that can be drawn from the data.

The size scale of the glinting area is indicated by the fringe visibility. Fig. 4 shows the square of the visibility, V^2, as a function of wavelength for the 5 s of data in which the fringe was detected. The decrease in V^2 at shorter wavelengths is a consequence of the higher resolution of the interferometer at shorter wavelengths alluded to in Section 2. If we assume that the glinting area of the solar panels is rectangular, we can calculate the expected V^2 as a function of λ, with the width of the glinting area as a free parameter.

The result of this fitting procedure is also shown in Fig. 4. The red curve shows best-fit width, 7.7 mas (37 nrad) corresponds to 1.34 m at the geostationary distance. A plausible range of widths is indicated by the blue curves. The upper curve corresponds to a width of 1.24 m (recall that a smaller object is less resolved and thus has a higher fringe visibility), while the lower curve corresponds to 1.44 m. The fact that we did not detect fringes on the 18.9 m AE-AC baseline is consistent with this width estimate: on the longer baseline, this width would produce $V^2 \sim 0.03$ at a wavelength of 850 nm, and smaller values at shorter wavelengths.
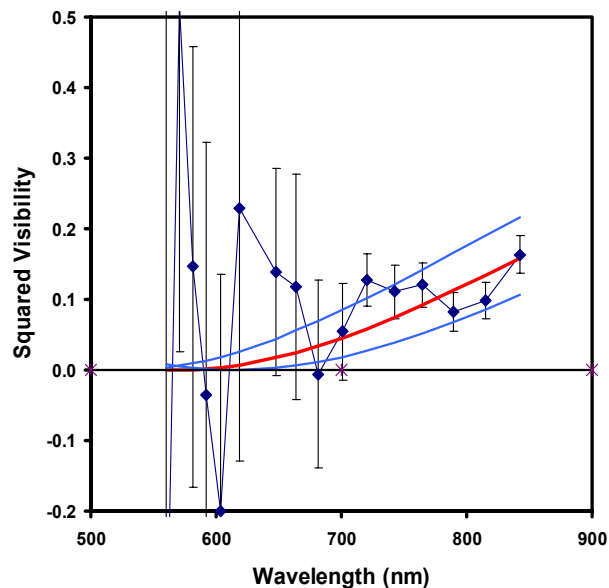

Fig. 4. Squared visibility vs. wavelength for DIRECTV-9S. The error bars emphasize the fact that the data are very noisy shortward of ~700 nm wavelength. The red curve shows the best-fit model of the glinting area, with a width of 1.34 m at the geostationary distance, or 7.7 mas (37 nrad), under the assumption that the area is rectangular. The blue curves give an indication of range of widths that the data could allow, from 1.24 m (upper curve) to 1.44 m (lower curve).

The NPOI data also produce an indication of the shape of the broadband spectrum of the satellite. Fig. 5 shows spectra from three of the nights on which we observed DIRECTV-9S. The red curves show the data from the NPOI baseline on which fringes were detected on 1 March, while the black curve shows data from the second baseline with no fringe detection. The data show that the satellite was somewhat redder when we detected the glint. The variation in the shape of the spectrum indicates that spectra alone may not be a good indication of target identification.

6. THE PROSPECT OF HIGH-PRECISION GEOSATELLITE POSITIONS

The astrometry that we carried out at the NOFS 40-inch telescope to support the interferometry experiment also served as an investigation of how precisely we can measure geosynchronous satellite positions. In monitoring the positions to pass on to the interferometer, we typically observed each satellite repeatedly over a period of half an hour to an hour. Although these satellites are geostationary, they do not appear completely motionless. An example

of the motion of one satellite, measured during our first run, October 2007, is shown in Fig. 6. These single-telescope observations show rms deviations from uniform motion of ~0.15 arcsec, indicative of the level of internal errors in our position measurements.
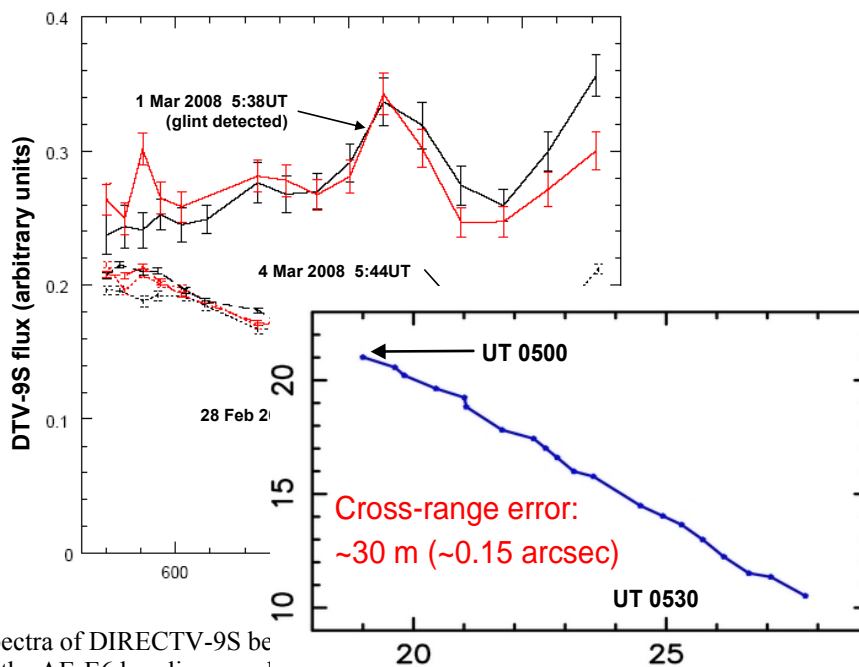

Fig. 5. Spectra of DIRECTV-9S be[...]
data from the AE-E6 baseline on w[...]
black curve shows data from the AE-AC baseline.

Position measurements with this level of precision, if carried out at two widely separated telescopes, suggest that the orbits of geostationary satellites can be measured to a high degree of precision. The internal error level of ~0.15 arcsec corresponds to a cross-range error of ~30 m at the geostationary distance. If positions of this accuracy are obtained at two telescopes separated by 1000 km, we can measure the range of the satellite by triangulation with an uncertainty of ~2 km.

During our second geosatellite run, in February and March 2008, we carried out position observations at both the Lowell Observatory 42-inch Hall telescope on Anderson Mesa (a few hundred meters from the NPOI) and at the NOFS 40-inch telescope, in part to quantify the external errors. We found that the internal errors are dominated by timing uncertainties. The satellites are nearly stationary in the sky, while the stars that form our positional reference system appear to move east to west at 15 arcsec per second of time. Therefore, we need to know the actual time at which an image is taken at the level of a few milliseconds to reduce the timing error below the internal positional errors, a level of accuracy that is not needed for normal stellar and planetary position measurements. The current timing errors are dominated by such effects as, for example, the time difference between issuing the command to open the shutter and the actual time of its opening. We are exploring a variety of software and hardware solutions to these problems.

7. PLANS

In the longer term, observing satellites with the NPOI requires improved sensitivity on short baselines. In this

Fig. 6. Position drift of a geostationary satellite measured at the NOFS 40-inch telescope on 14 October 2007. The axes are marked in arc seconds of elevation (vertical axis) and azimuth, offset from an elevation of 40º26´and azimuth 139º06´. The rms deviation from a straight line is ~0.15 arcsec, corresponding to 30 m at the

context, "short" means 15 m or less at visual wavelengths, or ~50 m or less at near-IR wavelengths. The 1.4 m CFRP telescope, which is light enough at ~230 kg (for the telescope and mount) to place on the current imaging station piers, offers the best prospect for a large increase of sensitivity on short baselines.

8. SUMMARY

We have used the Navy Prototype Optical Interferometer (NPOI) at visual wavelengths to observe a number of geostationary satellites during the "glint" seasons of October 2007, February-March 2008 and February-March 2009. Using a 15.9 m baseline of the NPOI, we succeeded in a tentative interferometric detection of one satellite, DIRECTV-9S, as it glinted to a brightness of 4th to 5th magnitude on 1 March 2008. Under some simple assumptions, the best-fit width of the glinting area is 1.34 m.

Our observations with the NPOI and the 40-inch Naval Observatory Flagstaff Station (NOFS) telescope also produced information. The shape of the satellite spectrum in the 500—800 nm data from the NPOI shows distinct changes over a period of days, suggesting that spectral characteristics are not always reliable as identifiers.

The positions we measured with the NOFS telescope to support the NPOI observations also suggest a technique for determining the positions of geostationary satellites with high precision. Our positional data show internal errors of ~0.15 arcsec, a level of precision that suggests that triangulation observations of satellites using telescopes separated by 1000 km could be used to measure geostationary satellite positions to a level of 30 m cross-range and 2 km along range.

9. REFERENCES

1. Schöller, M., Danchi, W. C., and Delplancke, F., Proc. SPIE Vol. 7013, *Optical and Infrared Interferometry*, SPIE, Bellingham, Washington, 2008.
2. Armstrong, J. T., et al., The Navy Prototype Optical Interferometer, Astrophys. J., Vol. 496, 550-571, 1998.
3. Hutter, D. J., et al., NPOI: recent progress and future prospects, Proc. SPIE, Vol. 7013, 701306, 2008.
4. Hummel, C. A., et al., A Co-phased Six-Station Optical Long-Baseline Array: Application to the Triple Star η Virginis, Astron. J., Vol. 125, 2630-2644, 2003.
5. Armstrong, J. T., et al., Diameters of δ Cephei and η Aquilae Measured with the Navy Prototype Optical Interferometer, Astron. J., Vol. 121, 476-481, 2001.
6. Peterson, D. M., et al., Vega is a rapidly rotating star, Nature, Vol. 440, 896-899, 2006.
7. Payne, T. E., and Gregory, S. A., Passive Radiometric Observations of Geosynchronous Satellites, IEEE Aerospace Conference Proceedings, Vol. 5, 2874-2884, 2004.
8. http://www.celestrak.com/NORAD/elements/geo.txt